Anatomy and Cell Biology Publications      Anatomy and Cell Biology Department

3-26-2010

# Neuropilin 1 directly interacts with Fer kinase to mediate semaphorin3A-induced death of cortical neurons

Susan X. Jiang
*National Research Council*

Shawn N. Whitehead
*Western University; National Research Council*, shawn.whitehead@schulich.uwo.ca

Amy Aylsworth
*University of Ottawa; National Research Council*

Bogdan Zurakowski
*National Research Council*

Kenneth Chan
*National Research Council*

*See next page for additional authors*

Citation of this paper:

Authors

Susan X. Jiang, Shawn N. Whitehead, Amy Aylsworth, Bogdan Zurakowski, Kenneth Chan, Jianjun Li, and Sheng T. Hou

# Neuropilin 1 Directly Interacts with Fer Kinase to Mediate Semaphorin 3A-induced Death of Cortical Neurons*[S]

**Susan X. Jiang**[‡], **Shawn Whitehead**[‡], **Amy Aylsworth**[‡§], **Jacqueline Slinn**[‡], **Bogdan Zurakowski**[‡], **Kenneth Chan**[¶], **Jianjun Li**[¶], and **Sheng T. Hou**[‡§1]

*From the* [‡]*Experimental NeuroTherapeutics Laboratory and* [¶]*Mass Spectrometry Glycoanalysis Laboratory, National Research Council (NRC) Institute for Biological Sciences, NRC Canada, Ottawa, Ontario K1A 0R6, Canada and the* [§]*Department of Biochemistry, Microbiology, and Immunology, University of Ottawa, Ontario K1H 8M5, Canada*

**Neuropilins (NRPs) are receptors for the major chemorepulsive axonal guidance cue semaphorins (Sema). The interaction of Sema3A/NRP1 during development leads to the collapse of growth cones. Here we show that Sema3A also induces death of cultured cortical neurons through NRP1. A specific NRP1 inhibitory peptide ameliorated Sema3A-evoked cortical axonal retraction and neuronal death. Moreover, Sema3A was also involved in cerebral ischemia-induced neuronal death. Expression levels of Sema3A and NRP1, but not NRP2, were significantly increased early during brain reperfusion following transient focal cerebral ischemia. NRP1 inhibitory peptide delivered to the ischemic brain was potently neuroprotective and prevented the loss of motor functions in mice. The integrity of the injected NRP1 inhibitory peptide into the brain remained unchanged, and the intact peptide permeated the ischemic hemisphere of the brain as determined using MALDI-MS-based imaging. Mechanistically, NRP1-mediated axonal collapse and neuronal death is through direct and selective interaction with the cytoplasmic tyrosine kinase Fer. Fer RNA interference effectively attenuated Sema3A-induced neurite retraction and neuronal death in cortical neurons. More importantly, down-regulation of Fer expression using Fer-specific RNA interference attenuated cerebral ischemia-induced brain damage. Together, these studies revealed a previously unknown function of NRP1 in signaling Sema3A-evoked neuronal death through Fer in cortical neurons.**

Injured central nervous system axons have a very limited capacity to regenerate due to the presence of a plethora of growth inhibitory ligands secreted from oligodendrocytes/myelin, reactive astrocytes, and fibroblasts in the damaged tissue (1–6). Neurons must integrate this multitude of inhibitory molecular cues, generated as a result of cortical damage, into a functional response. More often than not the response is one of growth cone collapse, axonal retraction, and neuronal death. Therefore, chemorepulsive factors likely contribute either directly or indirectly to neuronal death in the injured adult brain (7–10). Indeed, the expression of Sema3A, a major chemorepulsive factor, has been reported in several brain injury models, such as peripheral nerve injury, spinal cord injury, cerebral ischemia, and Alzheimer disease (1, 3, 11–16). In addition, Sema3A expression has been shown to increase vascular permeability, which may indirectly contribute to neuronal damage (17).

The biological activities of Sema3A during development are complex and context-dependent. Although best known for its role as an axonal growth cone repellent, Sema3A also serves as a chemoattractant during cortical layer development by guiding the radial migration of layer II/III cortical neurons (18) and the growth of apical dendrites toward the pial surface (19). In contrast, Sema3A is also important in stereotyped pruning of long hippocampal axon branches (20), causing dorsal root ganglia axon retraction (21), and evoking apoptosis of sensory neurons (22–24) possibly through activating apoptotic pathways involving PlexinA3 receptor and mitogen-activated protein kinases (25, 26).

The cellular receptors for semaphorins are neuropilins (NRP1 and NRP2)[2] (27, 28). Structurally, both NRPs contain an extracellular domain of two CUB motifs, adjacent to two domains with homology to coagulation factors V and VIII; a MAM domain; a single transmembrane domain; and a short intracellular domain of 39 amino acids lacking any known signaling motifs (27–29). The structural domain required for Sema3A/NRP1 interaction has been characterized (30), and several specific polypeptides antagonizing Sema3A IgG domain and NRP1 MAM domain have been found to inhibit Sema3A/NRP1-mediated inhibition of axonal outgrowth *in vitro* (31).

NRP1 is a multifunctional receptor, which mediates activities of structurally distinct ligands during development of the heart, vasculature, and neuronal system (32). An indication of the importance of NRP1 function in adult mice brain came from our recent discovery that NRP1 expression was transcriptionally regulated by the apoptosis-inducing transcription factor E2F1 (33). Activation of E2F1 causes neuronal death during

[2] The abbreviations used are: NRP1 and -2, neuropilins 1 and 2; MALDI-MSI, matrix-assisted laser desorption/ionization-mass spectrometry imaging; TOF, time of flight; MCAO, middle cerebral artery occlusion; PI, propidium iodide; RNAi, inhibitory RNA; Sema3A, semaphorin 3A; TTC, 2,3,5-triphenyltetrazolium chloride; TUNEL, terminal deoxynucleotidyltransferase dUTP nick end labeling; DIV, days *in vitro*; NMDA, *N*-methyl-D-aspartic acid; IP, immunoprecipitation.
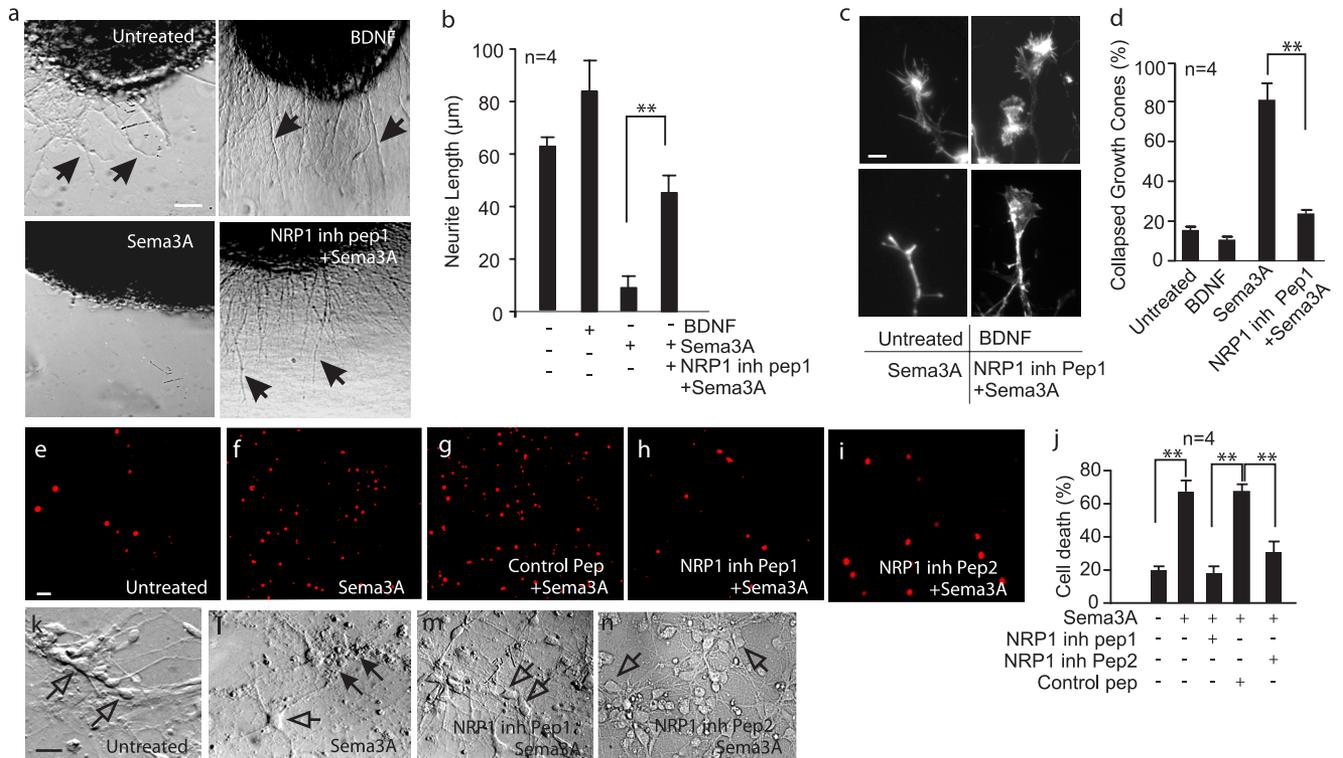
FIGURE 1. **NRP1 inhibitory peptide ameliorates Sema3A-mediated inhibition of neurite outgrowth, growth cone collapse, axonal damage and neuronal death.** Cortical brain tissue explants were cultured on a collagen matrix gel for 2–5 DIV, followed by treatment with brain-derived neurotrophic factor (50 ng/ml), or Sema3A (5 $\mu$g/ml) with or without pre-treatment with the NRP1 inhibitory peptide1 or the control peptide (20 $\mu$M) (*a–d*). Neurite outgrowth, as indicated by *solid arrows* in *a*, was measured using ImageJ on digitized images and plotted in *b*. Growth cone collapse induced by Sema3A treatment was visualized using phalloidin labeled with Alexa 488, and the representative images are shown in *c*. Increased number of collapsed growth cone and amelioration of growth cone collapse by NRP1 inhibitory peptide1 were quantified and plotted in *d*. To determine Sema3A-induced neuronal death, cortical neurons were cultured in the B27 and N2 supplemented neural basal medium for 7 DIV. These cells were untreated (*e*), treated with Sema3A (*f*), pretreated using the control peptide (*g*), NRP1 inhibitory peptide1 (*h*), or NRP1 inhibitory peptide2 (*i*). After 8-h incubation, PI (1 $\mu$g/ml) was added to the culture wells and incubated with cells for 30 min at 37 °C. Cells were examined under a florescence microscope to detect PI (*e–i*). The percentage of PI-positive cells were counted per 40× microscopic objective field and plotted in *j*. Changes in neurite morphology and length were shown in *k–n*. *Solid arrows* in *l* indicate dead cells, whereas *open arrows* in *k–n* indicate live cells under the phase-contrast microscope. *Error bars* = ±S.E. \*\*, statistical significance by one-way analysis of variance and further post hoc test for significant groups using Tukey's test with $p < 0.01$. Data were from at least three independent repeats. *Scale bars* = 20 $\mu$m.

cerebral ischemia (34, 35). In this study, the neuroprotective effects of blocking NRP1 interaction with Sema3A were investigated and the cytoplasmic tyrosine kinase Fer was determined as a downstream effecter for NRP1-mediated death signal transduction.

## EXPERIMENTAL PROCEDURES

*Cerebral Ischemia Produced by MCAO*—All procedures using animals were approved by the local Animal Care Committee (Protocol 2007.10). C57BL/6 mice (20–23 g) were obtained from Charles River (St Foie, Quebec). Under temporary isoflurane anesthesia, mice were subjected to middle cerebral artery occlusion (MCAO) using an intraluminal filament as previously described (36, 37). After 1 h of MCAO, the filament was withdrawn, and blood flow was restored to basal levels, as assessed by laser Doppler flowmetry. Wounds were sutured. The body temperature of experimental mice was monitored before and after the MCAO surgery using a rectal probe and was maintained at 37 °C using a heating pad and lamp. After 2, 4, 8, and 24 h and 2–7 days of reperfusion, mice were sacrificed. In preliminary experiments to verify a consistent stroke procedure, measurements of blood pressure, blood gases, and pH were also performed as previously described in both peptide-treated and small interference RNA-treated mice (38).

*Peptide Synthesis and Stereotactic Microinjection*—NRP1 inhibitory polypeptide 1 (NRP1 inh Pep1, targeting Sema3A IgG domain, HAVEHGFMQTLLKVTLE), NRP1 inhibitory polypeptide 2 (NRP1 inh Pep2, targeting NRP1 MAM domain, FWYHMSGSHVGTLRVKLP), and a sequence-scrambled control peptide (Control Pep, LKHEVMFLQETVTHLAG) were commercially synthesized (Genscript Corp., Piscataway, NJ) to a purity of 95% using high-performance liquid chromatography. Peptides (both the NRP1 inhibitory peptides and the control peptide) were dissolved in 0.01 M phosphate-buffered saline to a concentration of 2 mg/ml, and 5 $\mu$l was injected into the lateral ventricles (intracerebroventricularly) through stereotactical injection (Bregma, 0.9-mm lateral, 0.1-mm posterior, and −3.0-mm ventral) using a Hamilton microsyringe at 1 $\mu$l/min at a dosage of 0.4 mg/kg.

*MALDI-MSI of NRP1 Peptides*—Matrix-assisted laser desorption/ionization mass spectrometry imaging (MALDI-MSI) was used to detect distribution of NRP1 inhibitory peptides in the injected mouse brain as previously described (39, 40). Specifically, mice receiving unilateral MCAO and intracerebroventricular injections of the NRP1 inhibitory peptide were sacrificed 1 and 6 h after reperfusion. Entire intact mouse brains were removed carefully and flash frozen in liquid $N_2$. 10-$\mu$m coronal sections were cut using a cryostat, and the sections

were mounted onto pre-coated 41- × 41-mm stainless steel MALDI slides with a spray containing 10 mg/ml 2,5-dihydroxybenzoic acid DHB in 30% MeOH/$H_2O$. Each MALDI slide contained 300 $\mu$l of spray. The brain sections were then re-hydrated carefully with dd$H_2O$ mist. The mist effectively created a fog of moisture and provided a means to re-hydrate the sample without causing low molecular weight compound to shift. The re-hydrated sample was then sprayed with an additional 300 $\mu$l of 10 mg/ml 2,5-dihydroxybenzoic acid in 30% MeOH/$H_2O$ thus sandwiching the brain tissue sections between two layers of matrix. MALDI imaging was performed on an Applied Biosystems 4800 MALDI TOF/TOF. All analysis was done in positive ion using reflectron mode to obtain a high spectral resolution. The ionization was initiated with a third harmonic Nd:YAG pulse, and 75–150 spectra were then summed to provide 1 pixel on the image. The pitch of the pixels was between 75 and 100 $\mu$m. The instrument was controlled via a 4000 Series Imaging (Novartis, ABI). Data analysis and visualization were done using TissueView (ABI, Novartis).

*Fer RNAi Design, Transfection, and Intracerebroventricular Delivery in the Brain*—Stealth$^{TM}$ RNAi molecules were chemically modified, and blunt-ended, 25-mer double-stranded duplexes with minimal off-target effect were demonstrated by the manufacturer (Invitrogen). Chemically modified RNAi molecules (Stealth$^{TM}$ RNAi) targeting three different regions of mouse Fer kinase were designed and synthesized commercially by Invitrogen. A sequence-scrambled negative control Stealth$^{TM}$ RNAi duplex was also commercially synthesized by Invitrogen. Details of methods used, confirming the specificity of Fer, are described in the supplemental "Materials and Methods" (additional experimental procedures can also be found in the supplemental "Materials and Methods").

## RESULTS

*Sema3A Induces Neurite Retraction and Neuronal Death through NRP1 in Vitro*—To determine the role of Sema3A/NRP1 in adult cortical neurons, a synthetic polypeptide specifically inhibiting NRP1/Sema3A interaction (31) was chemically synthesized and used on cultured 7 DIV mouse cortical neurons. These neurons were treated with active Sema3A protein, which effectively induced significant neurite retraction and growth cone collapse in cultured cortical explants grown from embryonic (15 days) mice on a collagen matrix gel set on glass coverslips coated with poly-L-lysine (Fig. 1, *a–d*). The NRP1 inhibitory peptide1 effectively alleviated Sema3A-mediated inhibition of neurite outgrowth and growth cone collapse (Fig. 1, *a–d*). In contrast, brain-derived neurotrophic factor, serving as a positive control, significantly enhanced neurite outgrowth with fully extended growth cones shown by phalloidin staining (Fig. 1, *a–d*). These data demonstrated that NRP1 inhibitory peptide1 was effective in ameliorating Sema3A-mediated inhibition of neurite outgrowth.

We next sought to examine the effects of Sema3A on cortical neurons. Cortical cultures were deemed mature by 7 DIV due to their responsiveness to glutamate-induced excitotoxicity (supplemental Fig. S1). Interestingly, cortical neurons at 7 DIV treated with Sema3A resulted in neuronal death, as indicated by the increased number of propidium iodide (PI)-positive cells
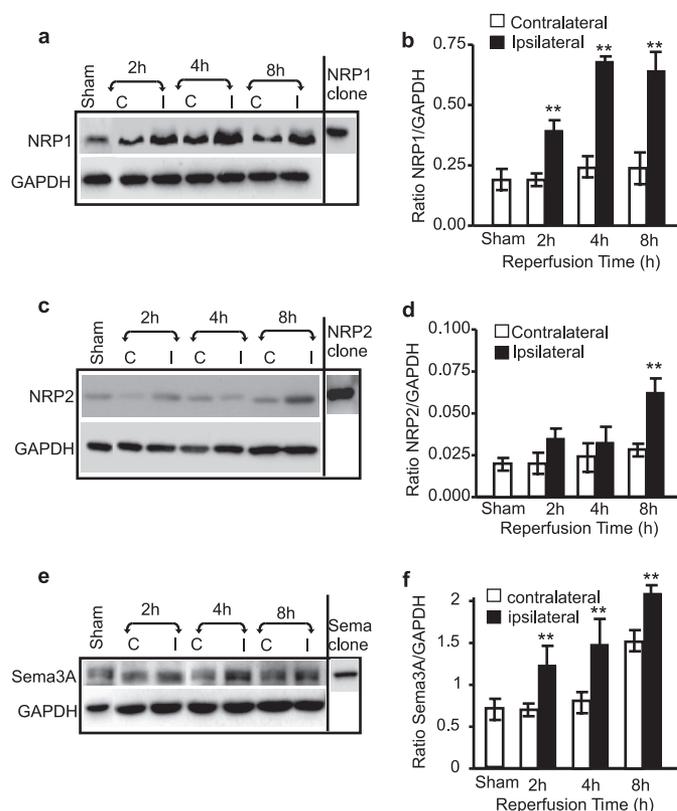


FIGURE 2. **Early induction in the expression of Sema3A and NRP1 in ischemic mouse brain.** Brains were removed from mice subjected to 1-h MCAO followed by 2-, 4-, or 8-h reperfusion. Proteins were isolated from both the contralateral (*C*) and ipsilateral (*I*) side of the brain. Western blotting was performed on 25 $\mu$g of brain protein to detect the expression of NRP1 (*a*), NRP2 (*c*), and Sema3A (*e*). The expression levels of NRP1, NRP2, and Sema3A were quantified against GAPDH (*b*, *d*, and *f*, respectively). A representative gel of at least three repeats is presented. **, statistical significance compared with the sham-operated group by one-way analysis of variance and further post hoc test for significant groups using Tukey's test with $p < 0.01$.

(Fig. 1, *f* and *j*). Sema3A-induced neuronal death was blocked by NRP1 inhibitory peptide1 (a peptide targeting the IgG domain of Sema3A) as compared with those neurons treated with the scrambled control peptide (Fig. 1, *g* and *j*). To determine the specificity of neuroprotection caused by blocking Sema3A/NRP1 interaction, NRP1 inhibitory peptide2 (targeting the MAM domain of NRP1) was also used. As shown in Fig. 1 (*i* and *j*), NRP1 inhibitory peptide2 was also significantly neuroprotective. Neurites in Sema3A-treated cortical neurons appeared short and fragmented as shown in Fig. 1*l* in comparison with the non-treated (Fig. 1*k*), and the NRP1 inhibitory peptide1- and 2-treated neurons (Fig. 1, *m* and *n*). Together, these studies demonstrated that Sema3A caused axonal damage and neuronal death of cortical neurons through interaction with NRP1 *in vitro* and that the synthetic NRP1 inhibitory peptides are specific and effective in preventing Sema3A toxicity.

*Increased Expression of Sema3A and NRP1 in Ischemic Mouse Brain*—To determine whether Sema3A/NRP1 are also involved in neuronal death in ischemic mouse brain *in vivo*, Western blotting was performed on mouse brain tissue subjected to MCAO. The expression of NRP1 increased 2 h after reperfusion, and its level remained high in the ischemic brain 8 h following reperfusion (Fig. 2, *a* and *b*). In contrast, the expression level of NRP2 did not change appreciably at 2 and

4 h after reperfusion but did demonstrate an increase 8 h following reperfusion (Fig. 2, *c* and *d*), indicating a late response of NRP2 in comparison with NRP1. Double immunostaining of brain sections showed that NRP1 expression was induced in neurons in response to ischemia (supplemental Fig. S2*a*), whereas NRP2 expression was barely detectable and only appeared along the lectin-positive microvessel wall (supplemental Fig. S2*b*). The expression of secreted Sema3A was also

increased in extracellular space (supplemental Fig. S2*c*) on the ipsilateral side of the ischemic brain (Fig. 2, *e* and *f*).

*NRP1 Inhibitory Peptides Are Neuroprotective in Vivo*—Based on the observation that Sema3A/NRP1 expression increased early in the ischemic brain, we hypothesized that inhibition of Sema3A/NRP1 is neuroprotective. NRP1 inhibitory peptide1 and -2, and the control peptide, were stereotaxically injected into the cerebral ventricles of mouse brains 1 h
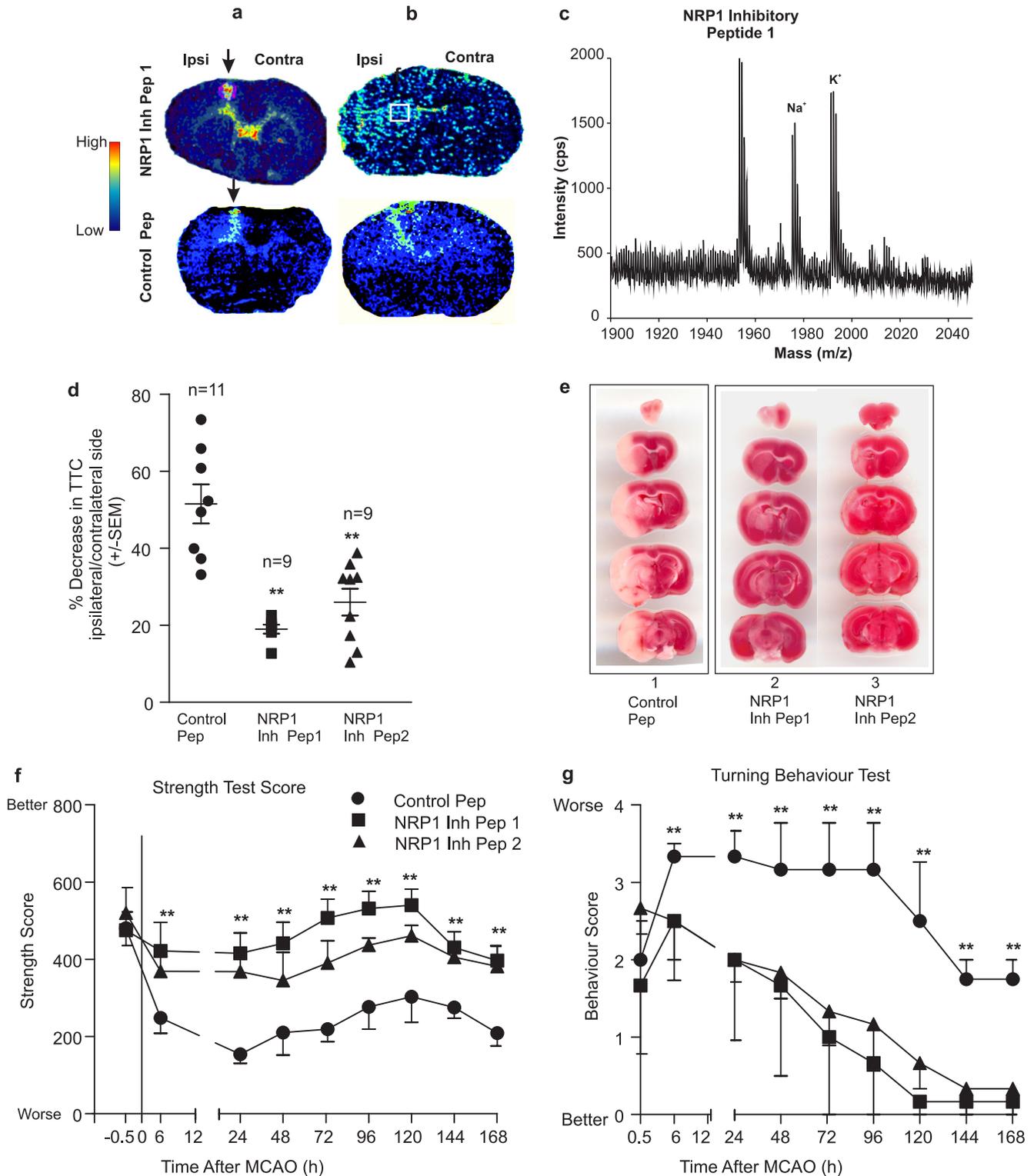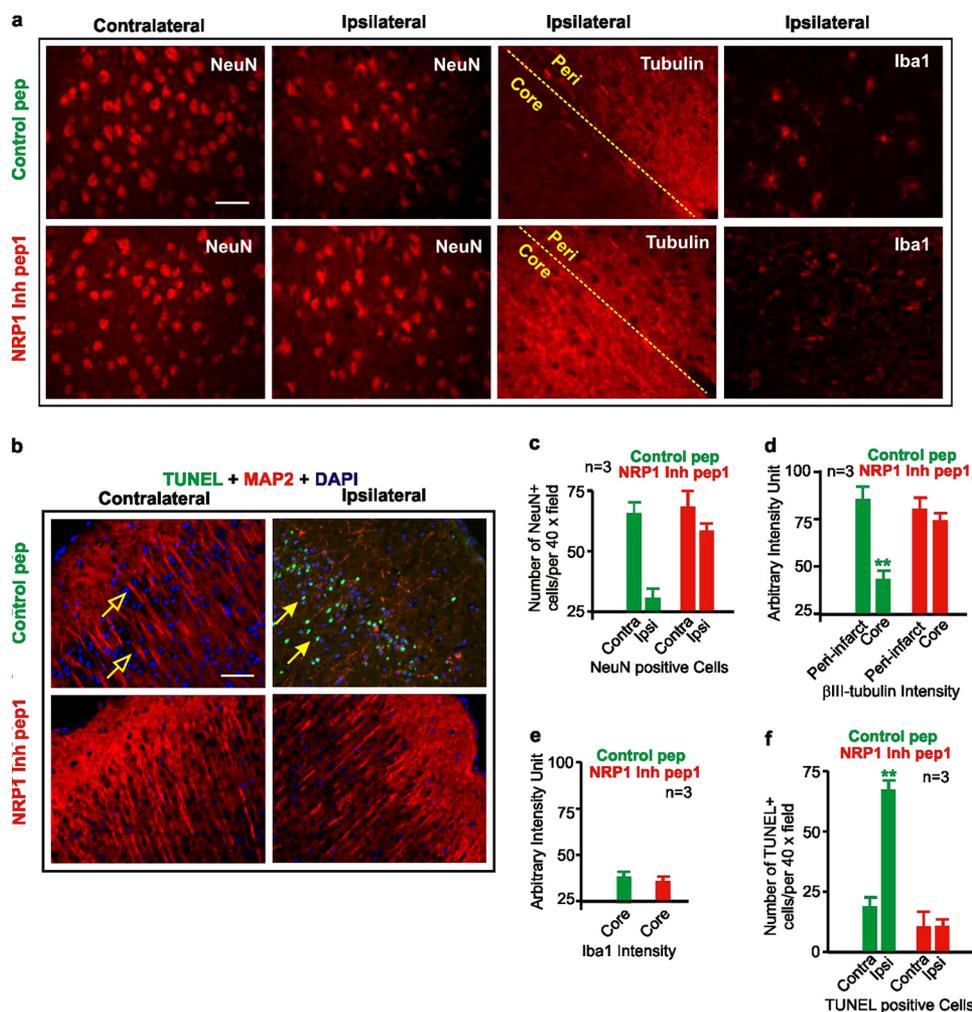
FIGURE 4. **Neuronal protection conferred by NRP1 inhibitory peptide.** MCAO mouse brains injected with the control peptide or the NRP1 inhibitory peptide1 were frozen-fixed and serially sectioned. Immunostainings for NeuN, $\beta$III-tubulin, and Iba1 (*a*) and double immunostaining with TUNEL and MAP2 were performed to show changes in NeuN positive neurons, microtubules in axons, the activated microglial cells and neuronal death in the ischemic brain, respectively (*b*). The *numbers* of NeuN-positive cells were counted from high resolution digital images (1300 × 1030 pixels) taken from in the ischemic cortex under a 40 × objective and plotted as shown in *c*. The intensity of $\beta$III-tubulin immunostaining was measured on digitized images taken from ischemic brains using the ImageJ software. An arbitrary intensity unit was used to show the relative changes in $\beta$III-tubulin intensity in the core and peri-infarct area of the brain (*d*). The intensity of Iba1 staining was also measured using the same method and shown in *e*. Brain sections adjacent to those used for NeuN staining were subjected to TUNEL and MAP2 double immunostaining (*b*). The number of TUNEL-positive cells per 40× objective field were counted and plotted in *f*. *Error bars* = ±S.E. Statistical significance was determined by the Mann-Whitney *U* test using data from at least three independent repeats. **, $p < 0.01$. *Scale bars* = 50 $\mu$m.

prior to MCAO followed by reperfusion for 24–168 h ($n = 9$ for NRP1 inhibitory peptides; $n = 11$ for the NRP1 control peptide). The body temperature before and after peptide injection, and during and after MCAO, were monitored using a rectal probe and maintained at 37 ± 2.5 °C. Body temperatures were found to be not significantly different between the NRP1 inhibitory peptides and NRP1 sequence-scrambled control peptide-injected mice. The body weight of these mice was also measured, which was at 23 ± 2 g before surgery and 20 ± 2 g at the time of sacrifice. No significant difference in weight loss occurred among the treatment groups, suggesting these peptides neither affect body temperature nor exacerbate body weight loss.

First, to determine whether the injected peptide maintained its integrity in the brain and to visualize the distribution of the injected peptide in the parenchyma, brain sections (10-$\mu$m thickness) were subjected to MALDI-MSI using the method as described under "Experimental Procedures." As shown in Fig. 3*a*, both NRP1 inhibitory peptide1 and the control peptide were found mostly along the injection needle tract (*arrow* in Fig. 3*a*) and in the lateral ventricles after 1-h MCAO. In contrast, after 6-h reperfusion, NRP1 inhibitory peptide and the control peptide signals were widely distributed in the ischemic side of the brain (Fig. 3*b*). MALDI-MSI analysis of the ischemic side of the brain showed that the injected

FIGURE 3. **Inhibition of NRP1/Sema3A interaction provides neuroprotection during cerebral ischemia.** Mice were injected with the control peptide or the NRP1 inhibitory peptide stereotactically into the lateral ventricles 1 h prior to a 1-h MCAO, followed by various reperfusion time. After 1-, 6-, and 24-h reperfusion, mice were killed and the brains were removed. Fresh frozen coronal brain sections (10 $\mu$m in thickness) were sectioned for MALDI-MSI (*a* and *b*; 1- and 6-h reperfusion, respectively) to demonstrate the increased dissemination of the injected peptide in the brain parenchyma. *Arrows* in *a* indicate the injection site and the presence of high level of the peptide along the needle track at 1 h after reperfusion. At 6 h after reperfusion, as shown in *b*, both the injected NRP1 inhibitory peptide1 and the control peptide were widely distributed in the parenchyma on the ischemic side of the brain (*ipsi* = ipsilateral side; *contra* = contralateral side). Total ion chromatograph of brain tissue from the *boxes* indicated in *b* (the *top panel*) depicts the spectrum of the NRP1 inhibitory peptide1 ($m/z$ 1952), as well as the Na$^+$ ($m/z$ 1975) and K$^+$ ($m/z$ 1991) ionized forms of the injected peptide (*c*). Brain infarction was measured using both a spectrophotometric-based method detecting soluble TTC color intensities extracted from the ischemic brains after 24-h reperfusion (*d*), and by staining the 2-mm thick coronal brain sections using TTC (*e*). *Lane 1* in *e* shows a representative image of serial coronal brain sections treated with the control peptide; *lanes 2* and *3* show representative images of brain infarctions from the NRP1 inhibitory peptide1- and 2-treated mice. During reperfusion, two motor behaviors were measured, including the forepaw grip strength test (*f*) and the six-point neurological deficit scores in turning behavior (*g*). *Symbols* in *panels f* and *g* are ● is for the control peptide, ■ for NRP1 inhibitory peptide1, and ▲ for NRP1 inhibitory peptide2. The total number of mice used were $n = 11$ for the control peptide-treated and $n = 9$ for both NRP1 inhibitory peptide1- and 2-treated mice. *Error bars* = ±S.E. Statistical analysis was performed to compare the control peptide and the NRP1 inhibitory peptide-treated brains using the non-parametric Mann-Whitney *U* test with ** indicating statistically significant at $p < 0.01$.

NRP1 inhibitory peptide1 was still intact with a molecular mass of 1954 Da matching the expected molecular mass of the original synthesized polypeptide (Fig. 3c). $Na^+$ and $K^+$ adducts of the NRP1 inhibitory peptide1 were also detected with masses of 1978 and 1992 Da, respectively, which were higher than the adduct-free NRP1 inhibitory peptide1.

Secondly, having established the fact that injected peptides were intact and effectively disseminated into the ischemic side of the brain, a series of experiments were performed to determine the neuroprotective effect of NRP1 inhibitory peptide. As shown in Fig. 3 (d–g), the NRP1 inhibitory peptide1 and -2 provided significant protection to MCAO-induced brain damage in comparison to the brain injected with the NRP1 control peptide, as measured by extraction of soluble TTC and quantification using a spectrophotometric-based measurement method (Fig. 3d, $p < 0.01$). TTC staining of 2-mm thick brain coronal sections was also shown in Fig. 3e to indicate the area of infarction. The neuroprotection by the NRP1 inhibitory peptide correlated with the significant improvement of motor functions as measured by 1) the forelimb grip strength test, which measures muscle strength and neuromuscular integration relating to the grasping reflex in the forepaws (Fig. 3f) and 2) a better performance in an expanded six-point neurological deficit turning behavior test (Fig. 3g). NRP1 inhibitory peptide1- and -2-treated mice performed significantly better after 6-h reperfusion ($n = 9$) in these tests compared with mice treated with the NRP1 control peptide ($n = 11$) (Fig. 3, f and g). The improvement of neurological functions was maintained at all the time points tested for up to 7 days after MCAO.

Finally, to validate that neurons were indeed protected by the NRP1 inhibitory peptide, immunostaining was performed on fixed brain sections. Significant reduction in βIII-tubulin staining occurred in neurons located in the infarct core of brains treated with the control peptide. In contrast, the expression level of βIII-tubulin was not significantly reduced in the NRP1 inhibitory peptide1-treated brain ($n = 3$, Fig. 4, a and d), suggesting protections to the neurite network and neurons. Correspondingly, the number of NeuN-positive neurons in the infarct core of NRP1 inhibitory peptide1-treated ischemic brains was also significantly higher than those in the control peptide-treated brain ($n = 3$, Fig. 4, a and c), suggesting that blocking Sema3A/NRP1 directly protected neurons during ischemia. The number of TUNEL-positive cells was also reduced significantly in NRP1 inhibitory peptide1-treated brains confirming that blocking Sema3A/NRP1 interaction reduced neuronal death (Fig. 4, b and f). To exclude the possibility that NRP1 inhibitory peptide1 may have an anti-inflammatory effect, immunostaining for activated microglia (antibody to Iba1 (Fig. 4, a and e)) was performed that demonstrated no significant changes in the levels of Iba1 expression in the infarct core or its surrounding peri-infarct tissue between the control and NRP1 inhibitory peptide1-treated mouse brains. These observations further support the idea that NRP1 directly mediates neuronal death in ischemic brain.

*Sema3A and NRP1 Inhibitory Peptide Do Not Affect NMDA-mediated Intracellular Calcium Influx into Neurons*—To address the mechanism by which NRP1 evokes neuronal death, and to exclude the possibility that NRP1 inhibitory peptide-
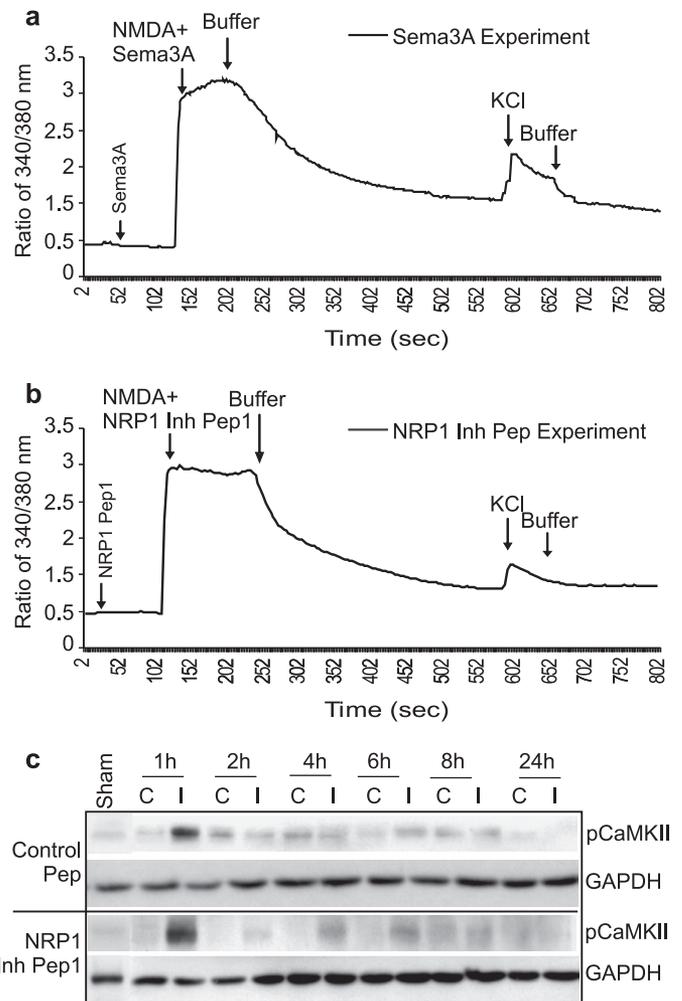


FIGURE 5. **NRP1 inhibitory peptide1 and Sema3A protein has no effect on $[Ca^{2+}]_i$ in cortical neurons.** The effect of 5 µg/ml Sema3A (a) and 20 µM NRP1 inhibitory peptide 1 (b) on $[Ca^{2+}]_i$ was determined by a ratiometric measurement of $[Ca^{2+}]_i$ using Fura-2 following procedures as described under "Experimental Procedures." $[Ca^{2+}]_i$ concentration was represented by the ratio of fluorescent intensity between the two wavelengths of $R_{340/380}$ of Fura-2 florescence. KCl (45 mM) and NMDA (100 µM) were used as controls to induce neuronal responses. Data were obtained from at least three independent experiments and the average of at least three experiments was plotted in a and b. Lines in a and b represent the averaged concentrations of $[Ca^{2+}]_i$. NRP1 inhibitory peptide1-treated and control peptide-treated ischemic brains were also collected for Western blotting to detect $[Ca^{2+}]_i$-evoked changes in pCaMKII (c). GAPDH protein was used as an internal loading control.

mediated neuroprotection was dependent of NMDA receptor function, we measured intracellular calcium ($[Ca^{2+}]_i$) changes in neurons, which are stimulated in response to NMDA activation. $[Ca^{2+}]_i$ influx in cortical neurons treated with Sema3A or NRP1 inhibitory peptide1, was measured using a Fura-2-based ratiometric measurement method as we previously described (36). Sema3A and NRP 1 inhibitory peptide alone did not evoke changes in $[Ca^{2+}]_i$ influx, nor did they affect NMDA-induced $[Ca^{2+}]_i$ influx (Fig. 5, a and b), excluding the possibility that NRP1 inhibitory peptide-mediated neuroprotection was through alteration of $Ca^{2+}$ channel functions during glutamate-induced excitotoxicity. In addition, early and rapid activation of pCaMKII following ischemia in response to glutamate-mediated $[Ca^{2+}]_i$ influx was also not affected by NRP1
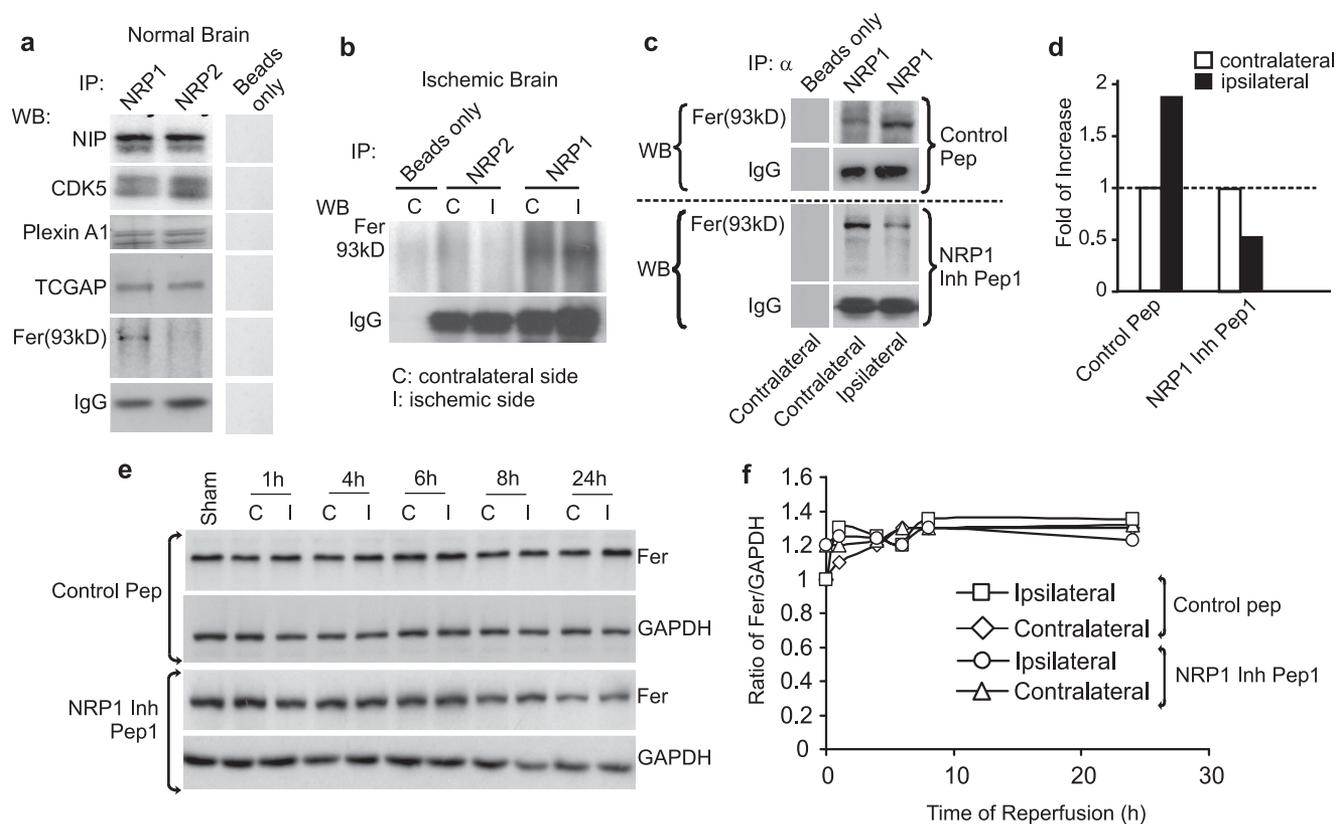
FIGURE 6. **NRP1 directly and selectively interacts with Fer in ischemic brains.** *a*, 200 $\mu$g of proteins from normal mouse brains were subjected to IP against NRP1 or NRP2. Equal amounts of IP products were subjected to Western blotting to detect NRP1 or NRP2 association with neuropilin-interacting protein, CDK5, Plexin A1, TCGAP, and Fer (*a*). In the IP reaction, a reaction without primary antibody was used as a negative control (*a*). To determine changes in Fer association with NRP1 during MCAO, ischemic brains were separated into contralateral (*C*) and ipsilateral (*I*) sides (*b*). Proteins from brain tissue were subjected to IP against NRP1 or NRP2. Western blotting was performed to detect Fer and IgG (as an internal control) as shown in *b*. The ischemic brains (200 $\mu$g) from both the NRP1 inhibitory peptide1-treated and the control peptide-treated mice were also subjected to IP against NRP1 (*c*). Western blotting was performed on these IP products to detect changes in Fer association with NRP1. IgG was used as a loading control. The intensities of the Fer band from two independent repeats were measured and quantified against those of the control peptide-treated brains shown in *d*. Total brain lysates were also subjected to Western blotting to detect the level of total Fer with GAPDH as an internal loading control (*e*). Densitometry measurements of band intensities were normalized against that of the sham-operated brain (*f*).

inhibitory peptide treatment (Fig. 5*c*), further supporting the fact that blocking Sema3A/NRP1 interaction did not affect $[Ca^{2+}]_i$. This result demonstrates that Sema3A/NRP1 signaling is independent of NMDA receptor functions.

*Fer Directly and Selectively Interacts with NRP1 in Ischemic Mouse Brain*—To identify the intracellular mediators of NRP1 signaling in neuronal death, immunoprecipitation (IP) was performed against NRP1 and NRP2 to identify molecules that directly and selectively interact with NRP1 during death signaling. The IP products derived from 200 $\mu$g of total brain proteins were subjected to Western blotting against neuropilin-interacting proteins, CDK5, Plexin A1, TCGAP, Fer, and Fer downstream-interacting protein, Cortectin (Fig. 6*a*; Cortectin is not shown). Surprisingly, only Fer (a cytoplasmic non-receptor tyrosine kinase) showed a selective association with NRP1, but not NRP2, in the IP products derived from the normal and ischemic mouse brain (Fig. 6, *a* and *b*). Next, we tested the hypothesis that the NRP1 inhibitory peptide1 treatment during MCAO would alter the level of association between NRP1 and Fer. Indeed, as shown in Fig. 6 (*c* and *d*), Western blotting of IP products against NRP1 showed that MCAO caused a 1-fold induction of association of Fer with NRP1 (Fig. 6*c*, *top panel*, and *panel d*), while NRP1 inhibitory peptide1

reduced Fer association with NRP1 in the ischemic brain by 1-fold (Fig. 6*c*, *bottom panel*, and *panel d*). Importantly, NRP2 did not interact with Fer either in the normal brain or in the ischemic brain (Fig. 6, *a* and *b*). Because the expression level of Fer in the ischemic brain did not change as seen on Western blot (Fig. 6, *e* and *f*), it is argued that it is the amount of association of existing Fer with NRP1 that is critical for NRP1 signal transduction.

Experiments were also performed to determine that the distal part of the NRP1 C-terminal domain is responsible for binding with Fer. The middle region of the cytoplasmic domain of NRP1 and NRP2 shares a high degree of homology in amino acid sequences. However, this region of high homology is not responsible for Fer binding. Using the deletion mutation studies, we found that the domain responsible for Fer binding is located within the last 18 amino acids toward the extreme C terminus of NRP1 where there is very low amino acid sequence homology between NRP1 and NRP2 (supplemental Fig. S3). Together with previous reports that overexpression of Fer caused death of non-neuronal cells and inhibited axonal outgrowth in neurons (41, 42), our studies strongly suggest that Fer interaction with NRP1 may lead to neuronal death.
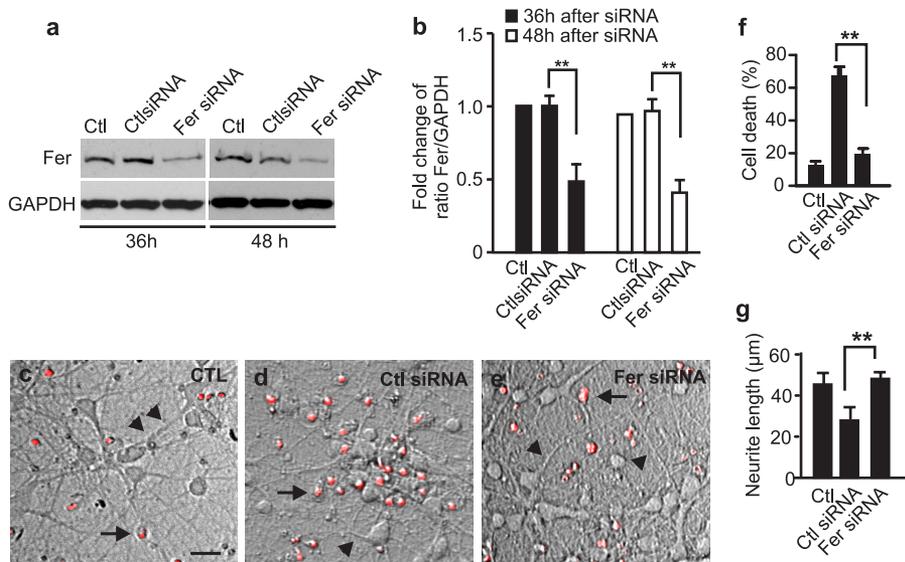
FIGURE 7. **Knocking down Fer using RNAi provides neuroprotection against Sema3A-induced toxicity in cortical neurons.** Cultured 7 DIV cortical neurons were transfected with Fer RNAi or its control negative RNAi at 1 $\mu$g/well in a 24-well plate. After 36- and 48-h transfection, cells were collected for Western blotting to demonstrate down-regulation of the expression of Fer as shown in *a*. GAPDH was detected on the Western blot and used as a loading control. Band intensity was measured using ImageJ, and the level of Fer was normalized against the level of GAPDH and plotted in *b*. After 36 h of Fer small interference RNA transfection, neurons were challenged with 5 $\mu$g/ml Sema3A. PI-positive cells, indicated by *long arrows*, are shown in *c–e*. The number of PI-positive cells was counted and plotted after 24 h of treatment (*f*). Neurite length, as indicated by *short arrows* in *c–e*, was also measured using ImageJ and plotted (*g*). At least 300 cells and their neurites were measured from at least three independent experiments. *Scale bar* in *c* = 50 $\mu$m. *Error bars* = ±S.E. Statistical significance was determined by one-way analysis of variance and further post hoc test for significant groups using Tukey's test with $p < 0.01$.

*Down-regulation of Fer Expression Confers Neuroprotection against Sema3A Toxicity in Vitro*—To demonstrate the direct role of Fer in mediating Sema3A/NRP1 response, a specific RNAi to Fer was designed and transfected in 7 DIV cortical neurons followed by treatment with Sema3A. As shown in Fig. 7 (*a* and *b*), Fer RNAi, but not the negative control RNAi, significantly reduced the Fer expression level in cortical neurons after 36 and 48 h. Interestingly, Fer RNAi-treated cortical neurons after 36 h in response to Sema3A (5 $\mu$g/ml, for 24 h) showed longer neurites and less neuronal death (PI-positive cells) when compared with the non-treated control and the negative control RNAi-treated neurons (Fig. 7, *c–g*). At least 300 cells and their neurites were measured from three independent experiments. These data demonstrate that Fer is directly involved in Sema3A/NRP1-mediated neuronal death.

*Down-regulation of Fer Expression Is Neuroprotective against MCAO in Vivo*—To further investigate whether Fer is an integral part of the signal transduction pathway in response to Sema3A-mediated neuronal death, a specific RNAi to Fer was used to down-regulate the expression of Fer during cerebral ischemia in mouse brain. The aim was to determine whether the reduction in Fer expression is neuroprotective. Fer expression is abundant in mouse brain as shown in Fig. 6*e* and Fig. 8*b* (*first lane*). Injection of chemically modified Stealth™ Fer RNAi in combination with invivofectamine™ transfection reagent allowed for efficient down-regulation of Fer protein level (more than 1-fold in reduction) in mouse brain between 48 and 72 h after injection (Fig. 8, *a–c*), whereas the control negative RNAi did not have any effect on the level of Fer expression (Fig. 8*b*, *lower panel*).

Based on the knockdown profile of Fer RNAi, mice were injected with Fer RNAi ($n = 7$) or the control negative RNAi ($n = 7$) for 48 h prior to the 1 h MCAO and 24 h reperfusion (Fig. 8*d* showing the experimental schema). Knocking down Fer expression using RNAi significantly reduced brain infarction size after 24-h reperfusion in comparison with the control negative RNAi-treated group (Fig. 8*e*). Specifically, Fer RNAi-treated brains showed a 23% reduction in infarct size compared with the control RNAi-treated group, which strongly suggests that the reduction in Fer expression is neuroprotective. Functionally, Fer RNAi-treated mice had a much better preservation of motor function as demonstrated by the significantly better forepaw grip strength scores (Fig. 8*f*) and neurological deficit scores (Fig. 8*g*) at 6- and 24-h reperfusion time points.

The neuroprotective effect of Fer knockdown was confirmed by immunohistochemical staining and TUNEL analysis (Fig. 9). MCAO caused a significant induction in the number of TUNEL-positive nuclei in the ischemic core in the control negative RNAi-treated mice (*arrows* in Fig. 9, *a* and *i*). Correspondingly, neurons in this area appeared to have a shrunken morphology, reduced numbers, and a low intensity of staining for NeuN (*open arrows* in Fig. 9, *c* and *j*). In contrast, Fer RNAi-treated mouse brains had significantly fewer TUNEL-positive nuclei (Fig. 9, *e* and *i*) and higher number of NeuN-positive cells (Fig. 9, *g* and *j*). Together, these studies showed that reducing Fer expression conferred neuroprotection to ischemic mouse brain.

In summary, these studies demonstrated that Sema3A expression causes death of adult cortical neurons and that blocking of Sema3A/NRP1 interaction is neuroprotective both *in vitro* and *in vivo*. Mechanistically, NRP1-mediated neuronal death was signaled directly through the cytoplasmic tyrosine kinase Fer.

## DISCUSSION

The present study revealed two very important findings: 1) the interaction between the chemorepulsive guidance molecule Sema3A and its receptor NRP1 is important in neuronal death both in cultured cortical neurons and during cerebral ischemia and 2) NRP1 directly interacts with the cytoplasmic non-receptor tyrosine kinase Fer to mediate neurite damage and neuronal death.

Although Sema/NRP's functions during development have been established (16, 18, 19, 43), their functions in the injured adult brains are just starting to be understood. Although several correlative studies have implicated semaphorins in a number of
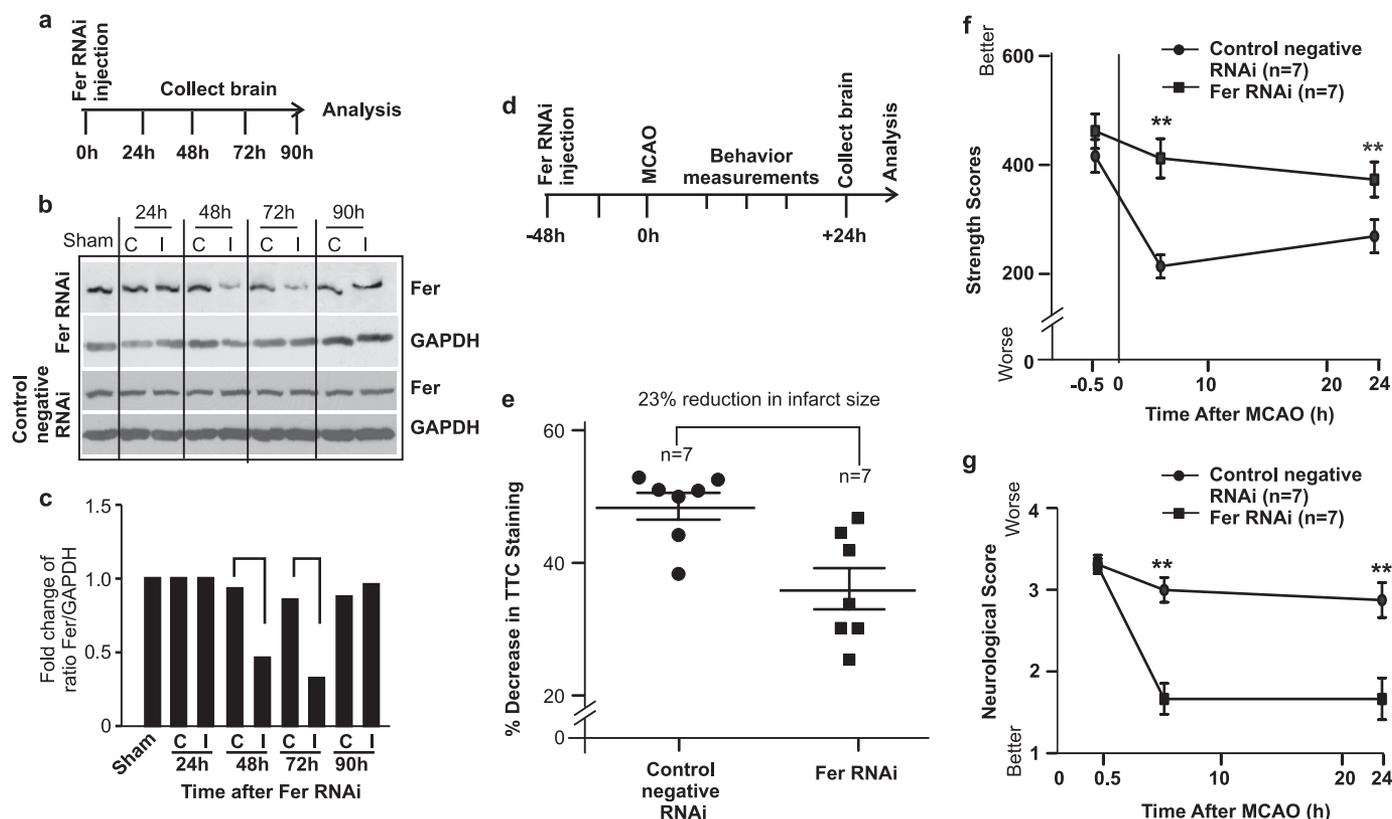
FIGURE 8. **Knocking down Fer is neuroprotective against MCAO-induced neuronal death and improves neurological functions.** *a*, schema of Fer RNAi delivery to mouse brain. Fer RNAi or the control negative RNAi was injected into mouse brains using stereotaxic injection. After 24, 48, 72, and 90 h of injection, mice were killed and brain was collected for protein extraction and Western blotting to detect changes in Fer expression level (*b*). Each brain was separated into the control side (*c*) and the injected side (*I*). Control mice were only subjected to skull surgery (labeled as *Sham* in *b*). The band intensities of Fer and GAPDH in Fer RNAi-injected mice brains were measured using ImageJ software, and the average -fold changes of the ratio of Fer/GAPDH of two repeat experiments were plotted (*c*). Fer protein level was reduced by more than 1-fold in brains after 48- and 72-h injection with Fer RNAi. Therefore, mice injected with Fer RNAi for 48 h were subjected to 1-h MCAO and followed by 24-h reperfusion. The experimental scheme is shown in *d*. Brain infarction size as indicated by the percentage of decrease in TTC staining between the ipsilateral and contralateral side of the ischemic brain was determined using a spectrophotometric-based method to detect soluble TTC color intensity extracted from the brain as described under "Experimental Procedures" (*n* = 7 for each treatment) and the result is shown in *e*. Forepaw grip strength test (*f*) and neurological deficit scores (*g*) were also performed before sacrificing the mice. *Error bars* = ±S.E. Statistical significance between the Fer RNAi-treated and control negative RNAi-treated groups was determined by a non-parametric Mann-Whitney *U* test with ** indicating *p* < 0.01.

neurodegenerative diseases, including Alzheimer disease, motor neuron degeneration, and injuries caused by cerebral ischemia (16, 44), direct evidence showing Sema3A-mediating neuronal death only comes from developmental evidence of sensory neurons (22, 24–26). An antibody to Sema3A has been shown to rescue retinal ganglion cells from cell death following optic nerve axotomy *in vivo* (23), and blocking Sema3A using a selective chemical inhibitor also enhanced nerve regeneration of transacted spinal cord in adult mice (15). Altogether, it is clear that inhibiting Sema3A may provide a therapeutic potential against neuronal death. What is not clear, however, is whether Sema3A function is occurring via NRP1 or NRP2, and perhaps more importantly what specific intracellular signals are being employed to mediate neuroprotection. In the present study, we used a synthetic peptide blocking Sema3A/NRP1 interaction to show successful neuroprotection both in cultured cortical neurons and in ischemic brains. The following evidence derived from this study demonstrated a direct causal relationship of Sema3A/NRP1 interaction with the death of adult cortical neurons: 1) Sema3A protein caused axonal growth cone collapse, axonal damage, and neuronal death positive to both PI and TUNEL staining; 2) NRP1 inhibitory peptides, capable of preventing Sema3A/NRP1 interaction, pre-

vented Sema3A-mediated neuronal death. Most importantly, Sema3A/NRP1 expression increased soon after ischemia reperfusion, and the NRP1 inhibitory peptides are neuroprotective to the brain during ischemia, suggesting the Sema3A/NRP1 pathway contributes to the acute cascade of deleterious biochemical events leading to ischemic neuronal death. Based on the expression profile of Sema3A/NRP1, the present study only examined the contribution of Sema3A/NRP1 after 24-h reperfusion. The long term benefit of blocking Sema3A/NRP1 interaction in ischemic brains remains to be investigated.

The MALDI-MS-based molecular imaging, although still in its infancy as a method, proved to be a novel and precise way to examine the integrity and distribution of the injected NRP1 inhibitory peptide (39, 45, 46). Using this method, we showed that NRP1 inhibitory peptide was able to cross the parenchyma following cerebral ischemia, presumably through the increased permeability of the blood-brain barrier as indicated by the higher level of signal in the ipsilateral side of the brain. NRP1 inhibitory peptide permeated a large area of the brain both in the cortex and striatum based on the MALDI-MSI data, which corresponds well with the area of MCAO-induced damage. This approach allowed a direct visualization of the integrity and distribution of the injected NRP1 inhibitor peptide and vali-
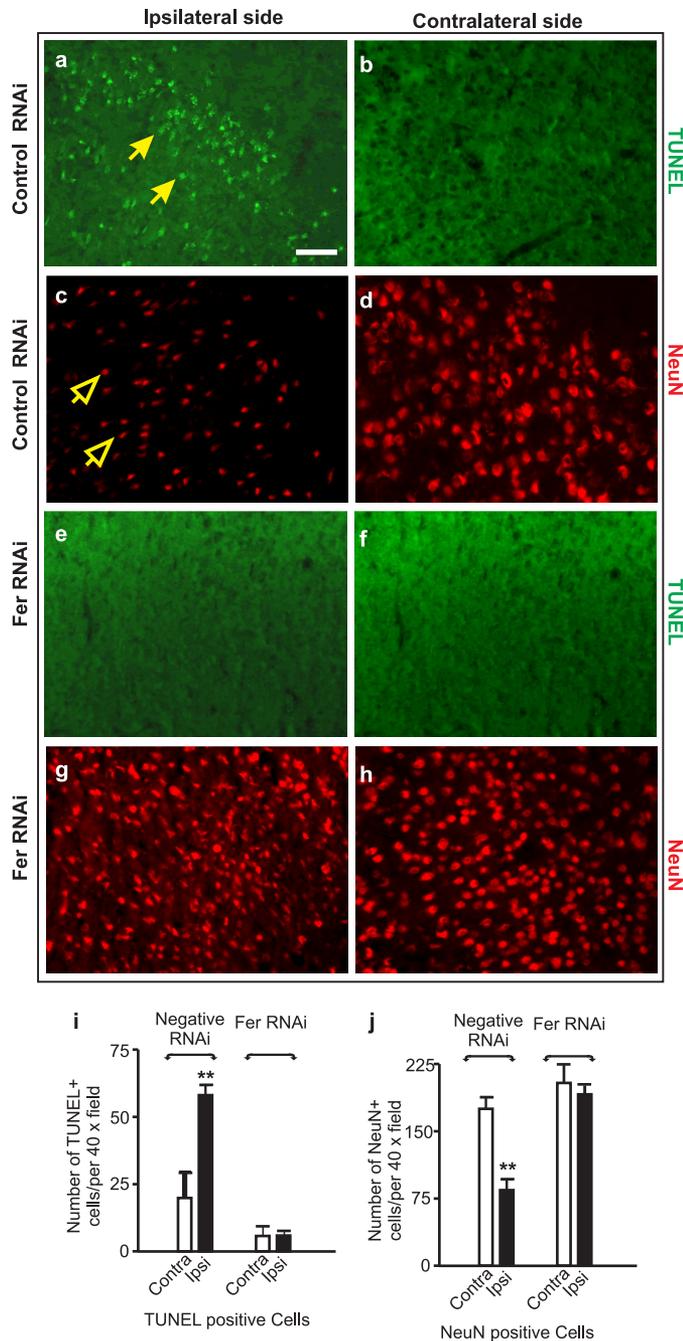
FIGURE 9. **Knocking down Fer expression reduces the number of TUNEL-positive neurons in ischemic mouse brain.** Mice injected with Fer RNAi for 48 h were subjected to 1-h MCAO, and followed by 24-h reperfusion. Mouse brains were subjected to frozen serial sectioning and immunostaining for TUNEL (*a, b, e,* and *f; solid arrows* in *a* indicate TUNEL-positive nuclei) and NeuN (*c, d, g,* and *h; open arrows* in *c* indicate NeuN-positive neurons). High resolution digital images of brain sections were taken, and the numbers of TUNEL- and NeuN-positive cells were counted on images covering the area of a 40× objective lens from the microscope (*i* and *j*). *Scale bar* = 80 $\mu$m. *Error bars* = ±S.E. Statistical significance was determined by a non-parametric Mann-Whitney *U* test with ** indicating $p < 0.01$ between the treated and control-treated groups using data from at least three independent repeats.

dated the findings that the neuroprotection observed in the NRP1 inhibitory peptide-treated brains was indeed due to the presence of the peptide.

Sema3A negatively affects the efficacy of synaptic transmission evoked in the CA1 region of hippocampal slices (47). From the current *in vitro* data, it is clear that NRP1 inhibitory peptide-mediated neuroprotection was independent of NMDA receptor-induced $[Ca^{2+}]_i$. The ratiometric $[Ca^{2+}]_i$ measurement showed that neither the NRP1 inhibitory peptide, nor Sema3A protein alone, had any effect on neuronal $[Ca^{2+}]_i$. Most importantly, addition of NRP1 inhibitory peptide or Sema3A protein did not affect NMDA receptor-mediated $[Ca^{2+}]_i$ influx into neurons as shown in Fig. 5, thereby excluding the possibility that NRP1-mediated neuronal death may be involved in coupling with NMDA receptors. These studies prompted us to search for NRP1-specific downstream effectors, of which there are not many known potential candidates to choose from. The cytoplasmic domain of NRP1 is relatively short, and it is believed that the C-terminal cytoplasmic domain of NRP1 is unable to mediate functional responses to Sema3A (48). However, surprisingly, based on an extended search for NRP1-selective interacting proteins using a co-immunoprecipitation approach, we found that Fer kinase was selectively associated with the NRP1 cytoplasmic domain. Most significantly, blocking Sema3A/NRP1 interaction with the specific synthetic inhibitory peptide reduced Fer binding to the NRP1 cytoplasmic domain. The reduction in Fer association with NRP1 cytoplasmic domain correlated well with neuroprotection. Together, these findings explain the selectivity of NRP1 in downstream signal transduction through Fer. Most interestingly, down-regulation of Fer expression is neuroprotective against Sema3A and cerebral ischemia as shown in Figs. 7–9, respectively. The fact that Fer$^{-/-}$ dorsal root ganglion neurons are not responsive to Sema3A (42) strongly indicates a role of Fer in neuronal response to Sema3A. This study, for the first time, clearly demonstrated that Fer is an important part of the death signal transduction pathway in adult cortical neurons. It remains unclear at this stage as to the downstream effectors for NRP1/Fer-mediated neuronal death, and they are currently being investigated. Possible candidates include collapsin response mediator proteins, which, we have previously shown, are important in mediating ischemic neuronal death (11, 33, 49).

In summary, the present study demonstrated a pivotal role for Sema3A/NRP1 in modulating the death of adult cortical neurons through direct and selective interaction with the cytoplasmic non-receptor tyrosine kinase Fer. Blocking Sema3A/NRP1 interaction is neuroprotective even during a relatively acute phase of stroke, firmly establishing Sema3A/NRP1/Fer as part of the damage response in acute stroke-induced neuronal death. Although the long term benefit of blocking Sema3A/NRP1 remains to be established, understanding this interaction provided a novel avenue to target non-NMDA receptors for development of therapeutics against stroke-induced brain damage.

## REFERENCES

1. De Winter, F., Oudega, M., Lankhorst, A. J., Hamers, F. P., Blits, B., Ruitenberg, M. J., Pasterkamp, R. J., Gispen, W. H., and Verhaagen, J. (2002) *Exp. Neurol.* **175,** 61–75
2. Giger, R. J., Pasterkamp, R. J., Holtmaat, A. J., and Verhaagen, J. (1998) *Prog. Brain Res.* **117,** 133–149
3. Pasterkamp, R. J., De Winter, F., Giger, R. J., and Verhaagen, J. (1998) *Prog. Brain Res.* **117,** 151–170
4. Pasterkamp, R. J., Giger, R. J., and Verhaagen, J. (1998) *Exp. Neurol.* **153,** 313–327
5. He, Z., and Koprivica, V. (2004) *Annu. Rev. Neurosci* **27,** 341–368
6. Yiu, G., and He, Z. (2006) *Nat. Rev. Neurosci.* **7,** 617–627
7. Deckwerth, T. L., and Johnson, E. M., Jr. (1993) *J. Cell Biol.* **123,** 1207–1222
8. Wakade, T. D., Palmer, K. C., McCauley, R., Przywara, D. A., and Wakade, A. R. (1995) *J. Physiol.* **488,** 123–138
9. Hou, S. T., Jiang, S. X., and Smith, R. A. (2008) *Int. Rev. Cell Mol. Biol.* **267,** 125–181
10. Raff, M. C., Whitmore, A. V., and Finn, J. T. (2002) *Science* **296,** 868–871
11. Hou, S. T., Keklikian, A., Slinn, J., O'Hare, M., Jiang, S. X., and Aylsworth, A. (2008) *Biochem. Biophys. Res. Commun.* **367,** 109–115
12. Beck, H., Acker, T., Püschel, A. W., Fujisawa, H., Carmeliet, P., and Plate, K. H. (2002) *J. Neuropathol. Exp. Neurol.* **61,** 339–350
13. Fujita, H., Zhang, B., Sato, K., Tanaka, J., and Sakanaka, M. (2001) *Brain Res.* **914,** 1–14
14. Pasterkamp, R. J., and Verhaagen, J. (2001) *Brain Res. Brain Res. Rev.* **35,** 36–54
15. Kaneko, S., Iwanami, A., Nakamura, M., Kishino, A., Kikuchi, K., Shibata, S., Okano, H. J., Ikegami, T., Moriya, A., Konishi, O., Nakayama, C., Kumagai, K., Kimura, T., Sato, Y., Goshima, Y., Taniguchi, M., Ito, M., He, Z., Toyama, Y., and Okano, H. (2006) *Nat. Med.* **12,** 1380–1389
16. Pasterkamp, R. J., and Giger, R. J. (2009) *Curr. Opin. Neurobiol.* **19,** 263–274
17. Acevedo, L. M., Barillas, S., Weis, S. M., Göthert, J. R., and Cheresh, D. A. (2008) *Blood* **111,** 2674–2680
18. Chen, G., Sima, J., Jin, M., Wang, K. Y., Xue, X. J., Zheng, W., Ding, Y. Q., and Yuan, X. B. (2008) *Nat. Neurosci.* **11,** 36–44
19. Polleux, F., Morrow, T., and Ghosh, A. (2000) *Nature* **404,** 567–573
20. Bagri, A., Cheng, H. J., Yaron, A., Pleasure, S. J., and Tessier-Lavigne, M. (2003) *Cell* **113,** 285–299
21. Gallo, G. (2006) *J. Cell Sci.* **119,** 3413–3423
22. Shirvan, A., Ziv, I., Fleminger, G., Shina, R., He, Z., Brudo, I., Melamed, E., and Barzilai, A. (1999) *J. Neurochem.* **73,** 961–971
23. Shirvan, A., Kimron, M., Holdengreber, V., Ziv, I., Ben Shaul, Y., Melamed, S., Melamed, E., Barzilai, A., and Solomon, A. S. (2002) *J. Biol. Chem.* **277,** 49799–49807
24. Gagliardini, V., and Fankhauser, C. (1999) *Mol. Cell Neurosci.* **14,** 301–316
25. Campbell, D. S., and Holt, C. E. (2003) *Neuron* **37,** 939–952
26. Ben-Zvi, A., Manor, O., Schachner, M., Yaron, A., Tessier-Lavigne, M., and Behar, O. (2008) *J. Neurosci.* **28,** 12427–12432
27. He, Z., and Tessier-Lavigne, M. (1997) *Cell* **90,** 739–751
28. Kolodkin, A. L., Levengood, D. V., Rowe, E. G., Tai, Y. T., Giger, R. J., and Ginty, D. D. (1997) *Cell* **90,** 753–762
29. Chen, H., Chédotal, A., He, Z., Goodman, C. S., and Tessier-Lavigne, M. (1997) *Neuron* **19,** 547–559
30. Antipenko, A., Himanen, J. P., van Leyen, K., Nardi-Dei, V., Lesniak, J., Barton, W. A., Rajashankar, K. R., Lu, M., Hoemme, C., Püschel, A. W., and Nikolov, D. B. (2003) *Neuron* **39,** 589–598
31. Williams, G., Eickholt, B. J., Maison, P., Prinjha, R., Walsh, F. S., and Doherty, P. (2005) *J. Neurochem.* **92,** 1180–1190
32. Gu, C., Rodriguez, E. R., Reimert, D. V., Shu, T., Fritzsch, B., Richards, L. J., Kolodkin, A. L., and Ginty, D. D. (2003) *Dev. Cell* **5,** 45–57
33. Jiang, S. X., Sheldrick, M., Desbois, A., Slinn, J., and Hou, S. T. (2007) *Mol. Cell. Biol.* **27,** 1696–1705
34. Hou, S. T., Callaghan, D., Fournier, M. C., Hill, I., Kang, L., Massie, B., Morley, P., Murray, C., Rasquinha, I., Slack, R., and MacManus, J. P. (2000) *J. Neurochem.* **75,** 91–100
35. MacManus, J. P., Jian, M., Preston, E., Rasquinha, I., Webster, J., and Zurakowski, B. (2003) *J. Cereb. Blood Flow Metab.* **23,** 1020–1028
36. Jiang, S. X., Lertvorachon, J., Hou, S. T., Konishi, Y., Webster, J., Mealing, G., Brunette, E., Tauskela, J., and Preston, E. (2005) *J. Biol. Chem.* **280,** 33811–33818
37. Weaver, J. G., Tarze, A., Moffat, T. C., Lebras, M., Deniaud, A., Brenner, C., Bren, G. D., Morin, M. Y., Phenix, B. N., Dong, L., Jiang, S. X., Sim, V. L., Zurakowski, B., Lallier, J., Hardin, H., Wettstein, P., van Heeswijk, R. P., Douen, A., Kroemer, R. T., Hou, S. T., Bennett, S. A., Lynch, D. H., Kroemer, G., and Badley, A. D. (2005) *J. Clin. Invest.* **115,** 1828–1838
38. MacManus, J. P., Koch, C. J., Jian, M., Walker, T., and Zurakowski, B. (1999) *Neuroreport* **10,** 2711–2714
39. Trim, P. J., Henson, C. M., Avery, J. L., McEwen, A., Snel, M. F., Claude, E., Marshall, P. S., West, A., Princivalle, A. P., and Clench, M. R. (2008) *Anal. Chem.* **80,** 8628–8634
40. Caprioli, R. M., Farmer, T. B., and Gile, J. (1997) *Anal. Chem.* **69,** 4751–4760
41. Rosato, R., Veltmaat, J. M., Groffen, J., and Heisterkamp, N. (1998) *Mol. Cell. Biol.* **18,** 5762–5770
42. Shapovalova, Z., Tabunshchyk, K., and Greer, P. A. (2007) *BMC Dev. Biol.* **7,** 133
43. Ding, S., Luo, J. H., and Yuan, X. B. (2007) *Biochem. Biophys. Res. Commun.* **356,** 857–863
44. De Winter, F., Holtmaat, A. J., and Verhaagen, J. (2002) *Adv. Exp. Med. Biol.* **515,** 115–139
45. Rohner, T. C., Staab, D., and Stoeckli, M. (2005) *Mech. Ageing Dev.* **126,** 177–185
46. Stoeckli, M., Chaurand, P., Hallahan, D. E., and Caprioli, R. M. (2001) *Nat. Med.* **7,** 493–496
47. Bouzioukh, F., Daoudal, G., Falk, J., Debanne, D., Rougon, G., and Castellani, V. (2006) *Eur. J. Neurosci.* **23,** 2247–2254
48. Tamagnone, L., and Comoglio, P. M. (2000) *Trends Cell Biol.* **10,** 377–383
49. Hou, S. T., Jiang, S. X., Desbois, A., Huang, D., Kelly, J., Tessier, L., Karchewski, L., and Kappler, J. (2006) *J. Neurosci.* **26,** 2241–2249